DOI: 10.1002/ejoc.200600719

Smaragdyrin–Azobenzene Conjugates: Syntheses, Structure, and Spectral and Electrochemical Properties

Sabapathi Gokulnath,[a] Viswanathan Prabhuraja,[a] Jeyaraman Sankar,[a] and Tavarekere K. Chandrashekar*[a][‡]

Keywords: Porphyrins / Dipyrromethane / UV/Vis spectroscopy / Isomerization / Electrochemistry

The syntheses, characterization, and spectral properties of smaragdyrin–azobenzene conjugates are reported. Our synthetic strategy involves linking the azobenzene group in one of the precursors to a dipyrromethane subunit, which was achieved by reaction of azobenzenecarbaldehyde with pyrrole under TFA catalysis. A [3+2] acid-catalyzed oxidative coupling of this precursor with the tripyrrane moiety gave the expected smaragdyrin–azobenzene conjugates. The azobenzene is in the (*E*) conformation both in the precursor and in the smaragdyrin conjugates, as revealed by its single-crystal X-ray structure. Electronic absorption and emission spectral studies reveal the presence of a moderate electronic interaction between the azobenzene and smaragdyrin π-systems. Irradiation experiments at 360 nm reveal the presence of a reversible (*E*)/(*Z*) transformation of the azobenzene moiety in the precursors **3b** and **4b**. However, in the smaragdyrin conjugates the formation of the (*Z*) conformer leads to the decomposition of the macrocycle upon prolonged irradiation. Excitation at the azobenzene absorption results in the appearance of the emission band of smaragdyrin, thereby suggesting an energy transfer. The electrochemical data reveal that ring oxidations of the smaragdyrin macrocycle become harder upon azobenzene introduction, which suggests the electron-withdrawing nature of the azobenzene in these conjugates. A significant shortening of the N–N bond (0.067 Å) and elongation of the C–N bonds (0.055 and 0.069 Å) in **7a** relative to the azobenzene–dipyrromethane precursor **4a** clearly reveal a rearrangement of the electronic π-delocalization pathway in the smaragdyrin–azobenzene conjugates. Rh^{I} binds to one amino and one imino nitrogen atom in the smaragdyrin cavity to form a 1:1 complex.

Introduction

Increasing attention has recently been devoted to materials containing photochromic azobenzene moieties because of interest in their application in fields such as photomemories,[1] optical switching,[2] and optoelectronics.[3] The introduction of azobenzene units into various molecular systems leads to an alteration in the properties of both the azobenzene and the molecular system.[4–6] This change in the properties can be utilized to build molecular photoswitches. Porphyrins[5] and phthalocyanines[6] are some of the most popular molecular systems for azobenzene linking. Specifically, azobenzene units are covalently linked either at the *meso* positions of porphyrin[5d] or through the *meso*-phenyl ring.[5a,5b] There are also examples where azobenzenes are linked through axial bonding involving a central metal ion coordinated to the porphyrin system.[5c] Very recently, Aida and co-workers[7] have reported a molecular system containing azobenzenes linked to (porphyrin)Zn complexes through a ferrocenyl spacer. They have shown that this system can, in principle, be used as a molecular motor due to a light-induced scissor-like conformational change that leads to the mechanical twisting of a noncovalently bound guest molecule. Thus, an understanding of the spectral, photochemical, and electrochemical properties of the ground and excited states is an important first step towards building photoresponsive molecular devices. Most of the systems studied in the literature are porphyrins and phthalocyanines. To the best of our knowledge, however, there are no reports on azobenzene-linked expanded porphyrin systems. The availability of larger delocalized π-electron systems and larger cavities in the expanded porphyrins[8] may lead to better interactions with the azobenzene partner relative to the simple porphyrin systems. Hence, in this paper we wish to report a series of smaragdyrin–azobenzene conjugates in which the azobenzenes are covalently linked at one of the *meso* positions of the 22π-electron smaragdyrin macrocycle. The spectral and electrochemical properties reveal a moderate electronic interaction between the smaragdyrin π-system and the azobenzene moiety, and it is shown that the azobenzene is in the (*E*) conformation in the conjugates.

[a] Department of Chemistry, Indian Institute of Technology, Kanpur 208016, India
Fax: +91-512-259-7436
E-mail: tkc@iitk.ac.in
[‡] Present address: Director, Regional Research Laboratory, Trivandrum, Kerala 695019, India
Supporting information for this article is available on the WWW under http://www.eurjoc.org or from the author.

Results and Discussion

Syntheses

The introduction of an azobenzene moiety at the *meso* position of smaragdyrin requires a precursor containing such a moiety. We therefore decided to introduce azobenzene into a dipyrromethane moiety, which is one of the precursors generally used for smaragdyrin synthesis.[9] This was achieved by performing the diazotization of *p*-aminobenzaldehyde (**1**) followed by coupling with phenol to give *p*-hydroxyazobenzenecarbaldehyde (**2**), which was further treated with methyl iodide and potassium carbonate in dmf to give the corresponding *p*-methoxy derivative **3**, which, on reaction with excess pyrrole under TFA catalysis, yielded the required dipyrromethane-containing azobenzene **4** (Scheme 1).

The synthesis of the smaragdyrins was achieved by the usual acid-catalyzed [3+2] oxidative coupling of **4a**,**b** with *para*-substituted 5,10-diphenyl-16-oxatripyrranes **5a**–**d**. The major products – the expected smaragdyrin–azobenzene conjugates – were isolated in about 25% yield (Scheme 2).[10] A trace amount of corrole was also formed in the reaction. The rhodium complexes were synthesized by treating the free base with di-μ-chloridobis[dicarbonylrhodium(I)] in the presence of sodium acetate[11] (Scheme 3). The purification was performed by silica gel chromatography. Complexes **8**–**11** were also found to be stable at room temperature. To the best of our knowledge, this is the first example of an expanded porphyrin containing an azobenzene moiety at the *meso* position.

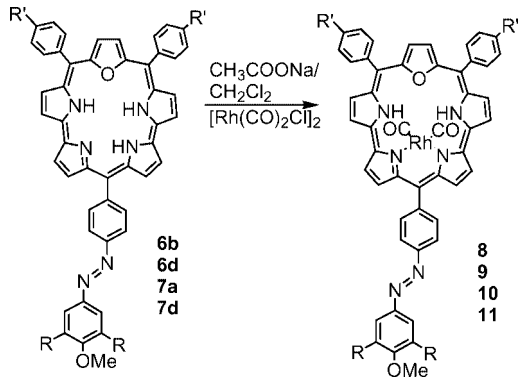

Scheme 3. Syntheses of rhodium complexes of azobenzene–smaragdyrin conjugates.

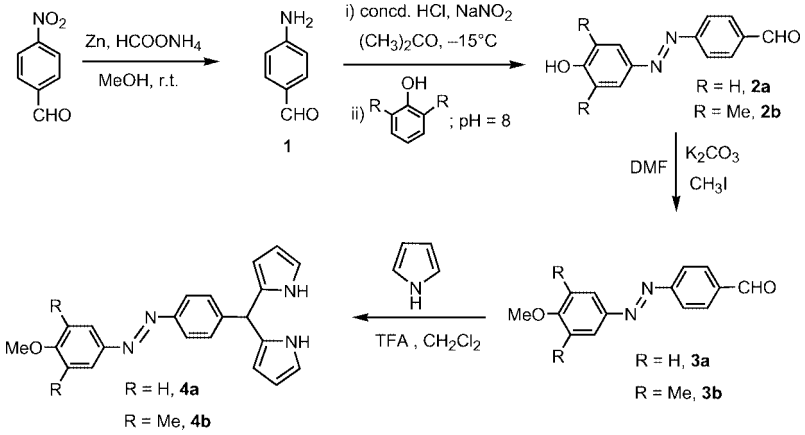

Scheme 1. Synthesis of dipyrromethanes **4a**,**b**.

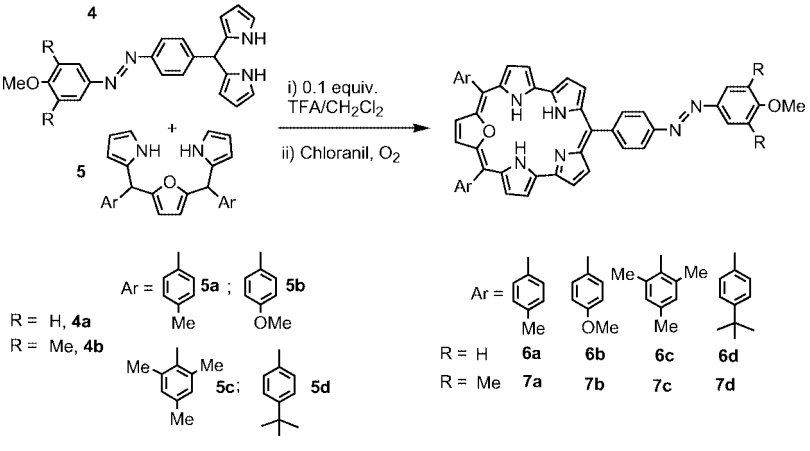

Scheme 2. Synthesis of azobenzene–smaragdyrin conjugates.

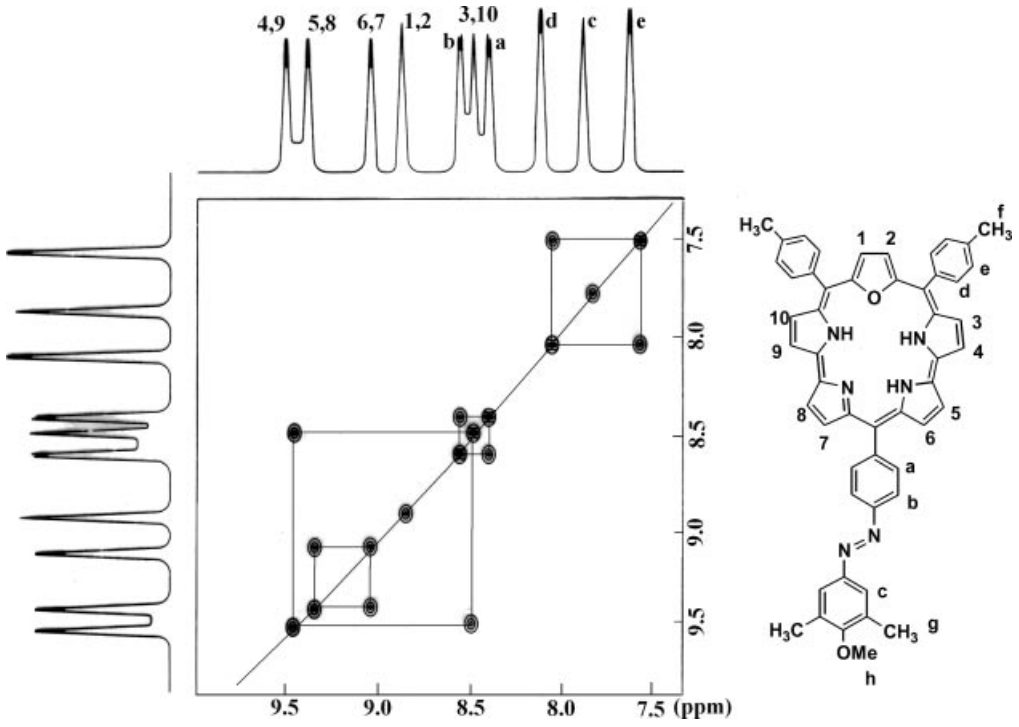

Figure 1. ^{1}H-^{1}H COSY spectrum of **7a** with assignments in the aromatic region.

The composition of the molecules was confirmed by FAB mass spectrometry and CHN analysis. The solution structure of the smaragdyrin was elucidated by detailed ^{1}H and 2D NMR studies. As a typical example, the ^{1}H and ^{1}H/^{1}H COSY spectrum in the aromatic region of **7a** is shown in Figure 1. The assignments and correlations observed are marked. The bipyrrole protons (3–10) resonate as four well-resolved doublets in the region δ = 8.5–10 ppm. The outer biyrrole protons (3, 6, 7, and 10) are more shielded as compared to the inner bipyrrole protons (4, 5, 8, and 9) because of the upfield ring-current contribution of the *meso*-aryl ring. The β-CH protons of the furan ring (1, 2) appear as a sharp singlet at δ = 8.8 ppm. Only two of the three inner NH protons are observed at room temperature (δ = –1.68 and –2.64 ppm). The third NH proton is involved in rapid tautomerism between the imino and amino nitrogen atoms at room temperature and hence is not seen. The observation of a singlet for the β-CH protons of the furan ring suggests a twofold symmetry bisecting the furan oxygen atom and the dipyrromethane unit. This is possible if the NH protons of the pyrrole in the dipyrromethane are exchanging with the nitrogen sites, thus supporting the presence of the tautomerism and being consistent with our earlier observation.[10] The presence of tautomerism was also confirmed by inserting Rh^{I} into the cavity. The ^{1}H NMR spectrum shows only one NH signal at δ = –1.89 ppm at room temperature, thus confirming the binding of Rh^{I} to the amino and imino nitrogen atoms, as observed previously by our group.[11]

The effect of azobenzene introduction on the expanded porphyrin skeleton is also observed in the ^{1}H NMR spectrum. For example, the chemical shifts of protons a and b attached to the azobenzene are deshielded by 1.06 and 0.86 ppm in **7a** relative to the dipyrromethane-containing azobenzene precursor **4b** (see Supporting Information). Furthermore, protons c and g experience a small deshielding, the extent of which depends on the distance of these protons from the porphyrin π-system.

Electronic Absorption Spectra

The electronic absorption spectra of **7a**, its rhodium complex **10**, and *meso*-tolylsmaragdyrin (**6e**) are shown in Figure 2. They show a typical intense Soret-like band in the region 440–460 nm and four Q-bands in the region 550–725 nm, thus confirming the porphyrin nature.[10] The UV/Vis data are listed in Table 1. The presence of the azobenzene chromophore is confirmed by the band at around 340 nm ($\varepsilon = 4 \times 10^4$ M^{-1} cm^{-1}), which is attributed to a π–π* transition in its (*E*) form.[5a] The introduction of azobenzene at the *meso* position results in the following changes in the absorption spectra: (a) a redshift and broadening and splitting of the Soret band (544 cm^{-1}); (b) a redshift (125–480 cm^{-1}) of the Q-bands; (c) on protonation both the Soret and Q-bands are redshifted and the number of Q-bands is also reduced, which is characteristic of *meso*-arylporphyrin systems[8] (see Supporting Information); (d) on metalation with Rh^{I} there is a 15-nm redshift in the Soret band and the Q-bands are also slightly redshifted; (e) the ε values of the metalated derivative are also reduced by 25–30%. These observations clearly suggest a weak electronic interaction between the azobenzene moiety and the porphyrin π-system.

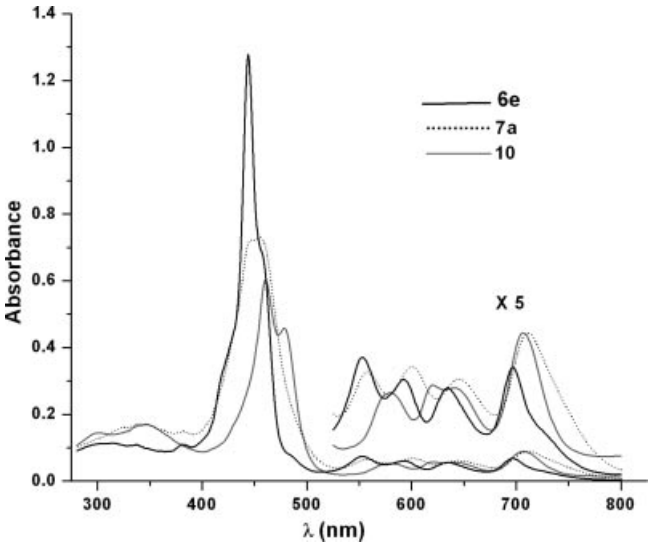

Figure 2. Electronic absorption spectra of **6e**, **7a**, and **10** in CH_2Cl_2 at a concentration of 0.5×10^{-6} M.

Table 1. UV/Vis absorption and emission data for smaragdyrin–azobenzene conjugates in dichloromethane.

	λ_{max} [nm] ($\varepsilon \times 10^{-4}$ [$M^{-1}cm^{-1}$])			λ_{em} [nm]
	Azo group	Soret	Q-bands	
6a	346 (4)	445 (21.3)	557 (2), 597 (1.7),	720
		456 (19.9)	641 (1.4), 707 (2.1)	
		445 (25)	555 (2.1), 595 (1.7),	721
6b	342 (3.8)	456 (19.7)	640 (1.4), 705 (2)	
		444 (21.5)	559 (2.7), 602 (2.7),	720
6c	343 (6.1)	456 (22.1)	647 (2.6), 719 (3.6)	
		445(28.1)	558(2.7), 601(2.8),	722
6d	349 (6.9)	456 (29.6)	647 (2.7), 715 (3.8)	
		444 (19)	556 (1.7), 597 (1.5),	721
7a	340 (4)	455 (19)	641 (1.2), 707 (1.9)	
		445 (19)	558 (1.9), 600 (2.1),	725
7b	346 (5.5)	456 (19.4)	647 (1.9), 712 (2.4)	
		444 (23.5)	559 (2.8), 602 (2.9),	721
7c	343 (6.8)	456 (23.9)	647 (2.7), 719 (3.9)	
		444 (33.6)	558(3.2), 601(3.2),	723
7d	344 (8.4)	455 (34.7)	647(3.0), 717(4.7)	
	297 (3.0)	460 (11.3)	579 (1.0), 618 (0.9),	724
8	346 (2.8)	478 (8.2)	639 (1.5), 704 (1.4)	
	300 (2.8)	461 (13.8)	579 (1.0), 619 (1.0),	722
9	351 (3.3.)	478 (10.5)	644 (1.0), 707 (1.7)	
	300 (3.5)	459(15.8)	578 (1.2), 618 (1.2),	724
10	345 (4.6)	477(11.8)	638 (1.8), 705 (2)	
	298 (3.8)	461 (17.3)	578 (1.3), 618 (1.3),	723
11	344 (4.6)	478 (13.2)	638 (1.3), 705 (2.3)	
			554 (2.3), 593 (2.3),	701
6e	–	444 (30)	634 (0.5), 695 (0.4)	

Irradiation Studies

The formation of (*E*) and (*Z*) isomers was monitored by irradiation experiments at approximately 360 nm for **7a** and the precursors **3b** and **4b**.[12] In the case of **7a**, irradiation at 360 nm resulted in a decrease in the absorption band centered at 350 nm and a small increase in the absorption band at 450 nm. A sharp decrease in intensity was also observed in the Soret region of the absorption spectra. These observations indicate the conversion of the (*E*) isomer into the (*Z*) isomer. However, upon continuous irradiation for approximately 5 min, the green color of the solution started to fade and the absorption spectrum of smaragdyrin completely disappeared, thus suggesting the decomposition of the complex. These observations prompted us to look into the (*E*)/(*Z*) isomerization process in the precursor aldehyde **3b** and dipyrromethane-containing azobenzene **4b**. Figure 3 shows the results of these experiments. Typically, irradiation at 360 nm results in a gradual decrease in the absorption at 350 nm with time and a small increase at about 450 nm, which suggests the presence of an (*E*)/(*Z*) conversion under photolytic conditions.

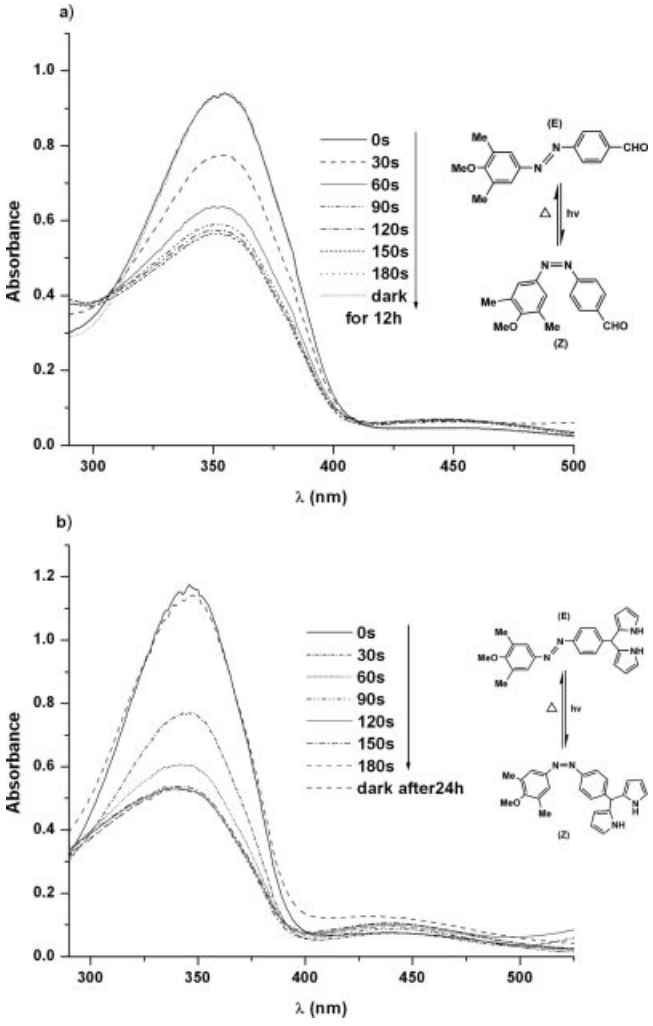

Figure 3. UV/Vis absorption spectral changes of the reversible (*E*)/(*Z*) isomerization of (a) **3b** and (b) **4b** in toluene. The irradiation time is shown in seconds.

These observations suggest the attainment of a photostationary state. The irradiated sample was kept in the dark for several hours, and the absorption spectra recorded after this time showed the emergence of a 350-nm band, thus suggesting the conversion of the (*Z*) into the (*E*) isomer in the dark. Thus, in precursors **3b** and **4b** the (*E*)/(*Z*) conver-

sion is reversible, while in the case of **7a**, even though (*E*)/(*Z*) isomerization takes place, the instability of the (*Z*) isomer results in the decomposition of the smaragdyrin macrocycle.

Emission Studies

The fluorescence spectra of smaragdyrin–azobenzene conjugates were recorded in toluene. Typically, excitation of the Soret band (444 nm) of smaragdyrin results in the observation of an emission band centered around 721 nm (Figure 4a). The emission data are listed in Table 1. A comparison of the emission spectrum of **6e**, which does not have an azobenzene substituent, with **7a** suggests a redshift of the emission maxima by about 20 nm followed by a broadening of the emission band. The full width at half maximum (FWHM) value for **7a** is 3261 cm^{-1}, which is 1.6-times higher than that of **6e**. These observations also suggest electronic communication between the azobenzene moiety and the porphyrin π-system. In order to prove the possible energy transfer from azobenzene to the porphyrin π-system, the fluorescence spectrum of **7a** was recorded by exciting at two different wavelengths. Thus, excitation at the Soret maximum (444 nm) resulted in the expected emission at around 721 nm, whereas excitation at 325 nm, which corresponds to the absorption of azobenzene, resulted in the appearance of a weak emission band (Figure 4a) with reduced intensity, which clearly suggests an energy transfer from the azobenzene moiety to the porphyrin π-system. A recent report from the Hecht group[13] also supports this energy-transfer hypothesis.

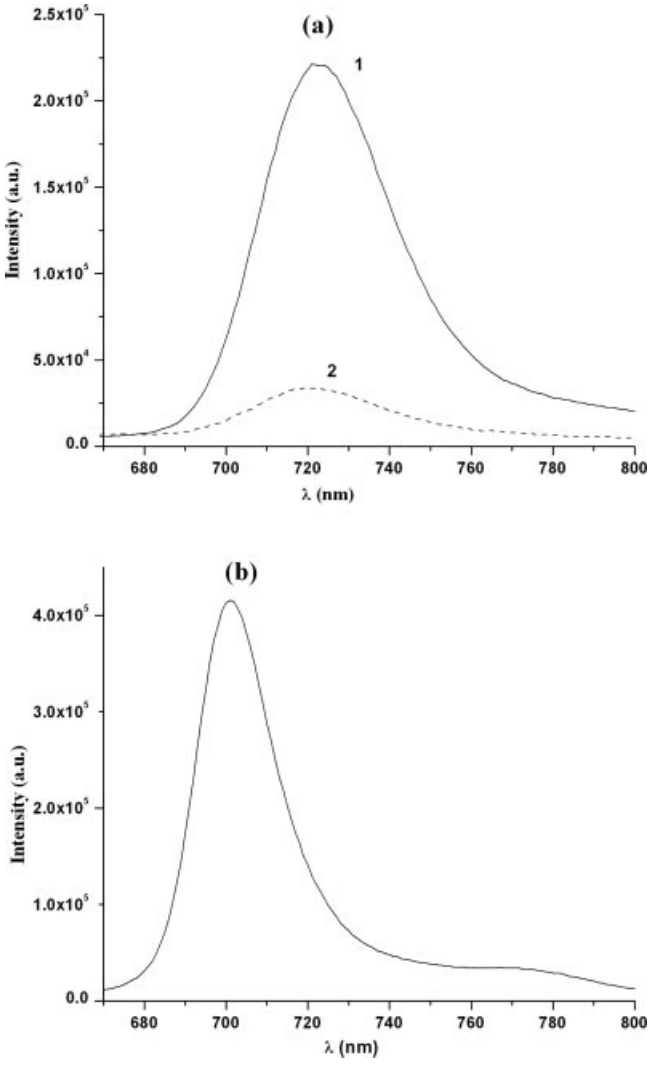

Figure 4. (a) Emission spectra of **7a** (bold line: λ_{exc} = 444 nm; dotted line: λ_{exc} = 325 nm); (b) emission spectrum of **6e** (λ_{exc} = 444 nm).

Electrochemical Studies

The redox behavior of the azobenzene-containing smaragdyrins was studied by cyclic voltammetry using 0.1 M tetra-*n*-butylammonium hexafluorophosphate ($TBAPF_6$) as supporting electrolyte in CH_2Cl_2, in the potential range –1.5 to 1.5 V vs. SCE. On scanning to negative potential, no proper reduction waves were observed. However, on scanning towards positive potential, two reversible oxidations corresponding to the smaragdyrin ring were observed for all the free bases and the Rh complexes. A comparison of the cyclic voltammogram of a smaragdyrin without an azobenzene moiety (**6e**) and one with an azobenzene moiety (**7a**) and its Rh complex (**10**) are shown in Figure 5. The differential pulse voltammogram is also shown. The electrochemical data are listed in Table 2. In all the cases two reversible oxidations ($\Delta E_p \approx$ 75–100 mV) were observed, except for **7c**, where the oxidations are quasi-reversible (ΔE_p = 120 mV). The introduction of azobenzene shifts the oxidation potential towards more positive values, which suggests more difficult oxidation. Finally, insertion of Rh^I into the smaragdyrin cavity further shifts the potentials towards more positive values. Earlier studies on porphyrins containing azobenzene revealed that the azobenzene moiety in these systems acts as an electron acceptor that attracts electron density from the porphyrin π-system.[5a] The observation of more difficult oxidations in the present study also reveals the electron-attracting nature of azobenzene in the smaragdyrin–azobenzene conjugates. Attempts to study the reduction of azobenzene in the negative potential region resulted in decomposition of the complex.

Table 2. Electrochemical data for azobenzene–smaragdyrin conjugates.

	6a	6b	6c	6d	6e	7a	7b	7c	7d	8	10
E^{ox1} [V]	0.368	0.345	0.396	0.384	0.329	0.349	0.343	0.403	0.390	0.412	0.428
E^{ox2} [V]	0.671	0.601	0.740	0.710	0.638	0.663	0.611	0.756	0.705	0.696	0.769

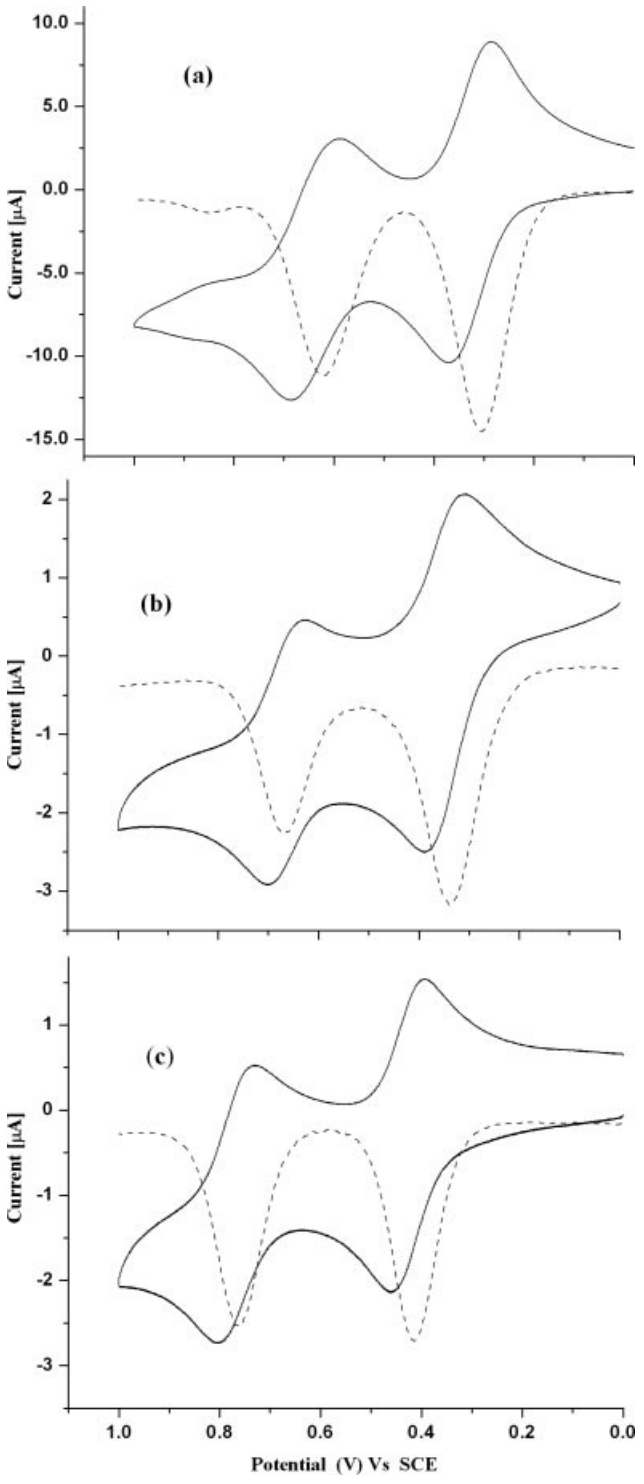

Figure 5. Cyclic voltammograms (solid line) and differential pulse voltammograms (dashed line) of (a) **6e**, (b) **7a**, and (c) **10** in CH_2Cl_2 containing 0.1 M $TBAPF_6$, recorded at a scan speed of 100 mV s^{-1}.

Crystallographic Characterization

In order to confirm the geometry of the azobenzene moiety in the smaragdyrin–azobenzene conjugates, the crystal structures of the precursor dipyrromethane-containing azobenzene **4a** and the smaragdyrin–azobenzene conjugate **7a** were solved. Selected crystallographic parameters are given in the Experimental Section. The structure of **4a** (Figure 6) clearly reveals the thermodynamically more stable azobenzene moiety in the (*E*) form. The azobenzene groups are almost perpendicular to the dipyrromethane moiety (dihedral angles of 69.04° for the pyrrole containing C1, C2, C3, C4, and N1 and 72.39° for the pyrrole ring containing C6, C7, C8, C9, and N2 with respect to the phenyl ring bonded to the dipyrromethane carbon). Compound **7a** (Figure 7) shows an almost flat structure with small deviations of the macrocycle from the mean plane. The mean plane is defined by the three *meso* carbon atoms C5, C14, and C23. These deviations are 18.19°, 11.21°, 6.83°, 12.95° for the pyrrole N1, N2, N3, and N4 rings, respectively, and 17.41° for the furan ring. The dihedral angle (58.75°) between the mean plane of the macrocycle and the *meso*-phenyl group of the azobenzene unit is slightly higher than that of the *meso*-tolyl group (51.05°, 42.27°). A molecule of methanol is trapped inside the cavity of the macrocycle and the side view of the structure clearly shows that the solvent methanol is held by two hydrogen-bonding interactions between the methanol oxygen atom and the hydrogen atoms attached to the pyrrole N1 and N4 rings (O3···H102 2.025 Å, 128.2°; O3···H103 2.121 Å, 94.97°). Some selected bond length data which reveal the changes in the electronic structure of the azobenzene moiety upon binding with smaragdyrin π-system are given in Table 3. For example, the length of the C14—C31 bond, which links the azobenzene moiety to the *meso* carbon atom, is reduced by 0.03 Å in **7a** compared to that in **4a**. On the other hand, the carbon–nitrogen bonds of azobenzene (C34—N5 and C37–N6) are longer in **7a** by 0.055 and 0.069 Å, respectively, relative to **4a**, thus clearly suggesting a change in the electron delocalization pathway. This is also supported by a significant reduction (0.067 Å) in the N–N bond length of the azobenzene moiety in **7a** compared to **4a**. These observations also

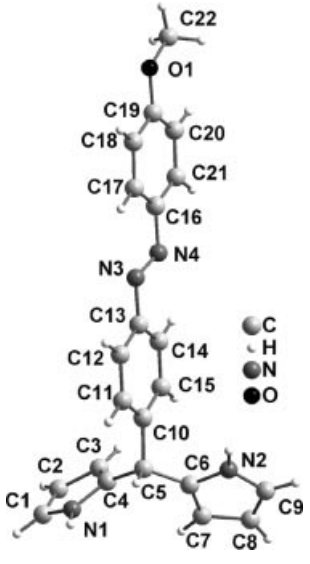

Figure 6. Single-crystal X-ray structure of **4a**.

confirm the electronic communication between the azobenzene moiety and the smaragdyrin π-system observed by spectroscopic studies.

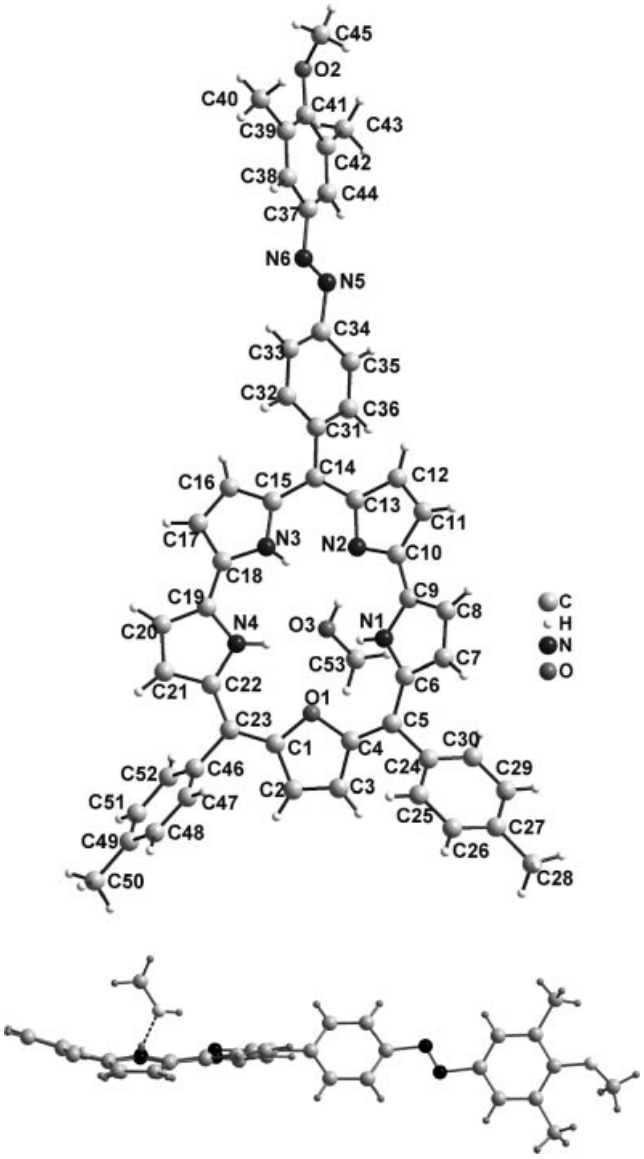

Figure 7. Single-crystal X-ray structure of **7a** with one trapped methanol molecule: (a) top view; (b) side view (*meso*-phenyl rings have been omitted for clarity; dotted lines show the hydrogen bond between methanol and the pyrrole NH groups).

Table 3. Selected bond lengths [Å] for **4a** and **7a**.

4a		**7a**	
C5–C10	1.526(2)	C14–C31	1.495(5)
C13–N3	1.427(2)	C34–N5	1.479(7)
C16–N4	1.423(2)	C37–N6	1.496(7)
N3–N4	1.258(2)	N5–N6	1.191(5)

Conclusions

We have synthesized smaragdyrin–azobenzene conjugates by [3+2] acid-catalyzed oxidative coupling of the appropriate precursors. The spectroscopic and electrochemical measurements clearly show that the azobenzene moiety directly covalently linked to the *meso* carbon atom of the macrocycle leads to a moderate interaction between the azobenzene moiety and the macrocyclic π-system. These studies also reveal partial electron transfer from smaragdyrin to the electron-withdrawing azobenzene moiety and energy transfer from the azobenzene moiety to the smaragdyrin π-system. The facile reversible (*E*)/(*Z*) isomerization for azobenzene-containing precursors **3b** and **4b** has been demonstrated by irradiation studies. Similar attempts were also made for the smaragdyrin–azobenzene conjugates. The solid-state structures of **4a** and **7a** further confirmed the proposed structure, where azobenzene is in its (*E*) form. Efforts to prepare a series of covalently linked azobenzene moieties with other expanded porphyrins and to study their coordination chemistry are currently underway in our group.

Experimental Section

Instrumentation: Electronic spectra were recorded with a Perkin–Elmer Lambda 20 UV/Vis spectrophotometer. ^{1}H NMR spectra were recorded with a 300 MHz JEOL spectrometer with samples in $CDCl_3$. FAB mass spectra were recorded with a JEOL-SX-120/DA6000 spectrometer. The fluorescence spectra were recorded with a SPEX-Fluorolog F112X spectrofluorimeter. Cyclic voltammetric studies were performed with a CH instrument (CH, 620B). A three-electrode system consisting of a platinum working electrode, a platinum mesh counter electrode, and a commercially available saturated calomel electrode (SCE) as the reference electrode were used. Irradiation studies were carried out using the output from a 200-W high-pressure mercury lamp, which was passed through a 360-nm Oriel band-pass filter.

Chemicals: All NMR solvents were used as received. Solvents like dichloromethane, tetrahydrofuran, and *n*-nexane were purified and distilled by standard procedures. Tetra-*n*-butylammonium hexafluorophosphate from Fluka was used as the supporting electrolyte for cyclic voltammetric studies. 2,5-Bis[hydroxy(phenyl)methyl]-furan and 5,10-diphenyl-16-oxatripyrranes **5a**–**5d** were prepared according to the published procedure[14] and stored under an inert gas at –10 °C.

4-Aminobenzaldehyde (1): 4-Aminobenzaldehyde (**1**) was prepared by suitable modification of a literature method.[15] A suspension of 4-nitrobenzaldehyde (7.6 g, 50 mmol) and Zn dust (3.9 g, 60 mmol) was stirred with ammonium formate (4.7 g, 75 mmol) at room temperature. The reaction was monitored by TLC and, after completion of the reaction, the mixture was filtered. The organic phase was washed successively with brine, water (2 times), and dried with Na_2SO_4. The solvent was removed under reduced pressure to afford **1** as an orange semi-solid (yield: 4.8 g, 80%).

4-Formyl-4′-hydroxyazobenzene (2a): A solution of 4-aminobenzaldehyde (**1**) (4.8 g, 40 mmol) in acetone (40 mL) was added to a stirred mixture of concd. HCl (7 mL in 20 mL of water) at –15 °C. $NaNO_2$ (2.7 g in 15 mL water, 39 mmol) was added dropwise to this solution and stirring was continued for 15 min. A solution of phenol (3.73 g, 40 mmol) in 30 mL of 10% NaOH was added very slowly to the diazonium salt solution over a period of 20 min. The color of the solution changed from orange to red and the mixture was stirred for a further 30 min to attain room temperature. The organic phase was extracted with CH_2Cl_2, washed with $NaHCO_3$,

and dried with Na_2SO_4. The solvent was removed in a rotary evaporator and the resulting red solution was purified by column chromatography [silica gel (100–200 mesh), ethyl acetate/petroleum ether, 20:80]. The first moving orange fraction was identified as containing 4-formyl-4′-hydroxyazobenzene (**2a**). Yield: 3.2 g (35%). FAB-MS: *m/z* (%) = 226 (100) [M$^+$]. ^{1}H NMR (300 MHz, $CDCl_3$, 25 °C, TMS): δ = 7.02 (d, J = 9 Hz, 2 H), 7.95 (m, 6 H), 10.09 (s, 1 H) ppm. $C_{13}H_{10}N_2O_2$ (226.23): calcd. C 69.02, H 4.46, N 14.14; found C 69.12, H 4.36, N 14.21. This procedure was repeated with 2,6-dimethylphenol instead of phenol to synthesize **2b**.

Compound 2b: FAB-MS: *m/z* (%) = 254 (100) [M$^+$]. ^{1}H NMR (300 MHz, $CDCl_3$, 25 °C, TMS): δ = 2.35 (s, 6 H), 7.62 (s, 2 H), 8.03 (m, 4 H), 10.09 (s, 1 H) ppm. $C_{15}H_{14}N_2O_2$ (254.28): calcd. C 70.85, H 5.55, N 12.58; found C 70.63, H 5.72, N 12.47.

4-Formyl-4′-methoxyazobenzene (3a): A solution of **2a** (3 g, 13 mmol) in dmf (30 mL) was added dropwise to a suspension of K_2CO_3 (3.7 g, 27 mmol) in dmf (15 mL) and the mixture stirred under N_2 for 30 min. CH_3I (1.65 mL, 27 mmol) was added dropwise to this solution at 0 °C. The resulting mixture was stirred at room temperature for 24 h and poured onto crushed ice to remove excess K_2CO_3 and dmf. The organic phase was extracted with CH_2Cl_2 (5 × 150 mL), washed twice with water, and dried with Na_2SO_4. The solvent was removed in a rotary evaporator and the resulting orange solution was purified by column chromatography [silica gel (100–200 mesh), ethyl acetate/petroleum ether, 8:92]. The first moving orange fraction was identified as containing 4-formyl-4′-methoxyazobenzene (**3a**). Yield: 2.1 g (65%). FAB-MS: *m/z* (%) = 241 (90) [M$^+$]. ^{1}H NMR (300 MHz, $CDCl_3$, 25 °C, TMS): δ = 3.89 (s, 3 H), 7.02 (d, J = 9 Hz, 2 H), 7.98 (m, 6 H), 10.08 (s, 1 H) ppm. $C_{14}H_{12}N_2O_2$ (241.26): calcd. C 69.99, H 5.03, N 11.66; found C 69.86, H 5.28, N 12.01. This procedure was repeated with **2b** to synthesize **3b**.

Compound 3b: FAB-MS: *m/z* (%) = 268 (100) [M$^+$]. ^{1}H NMR (300 MHz, $CDCl_3$, 25 °C, TMS): δ = 2.39 (s, 6 H), 3.80 (s, 3 H), 7.66 (s, 2 H), 8.01 (s, 4 H), 10.09 (s, 1 H) ppm. $C_{16}H_{16}N_2O_2$ (268.21): calcd. C 71.62, H 6.01, N 10.44; found C 71.89, H 5.85, N 10.21.

Compound 4a: A mixture of pyrrole (14.4 mL, 0.21 mol) and **3a** (2 g, 8.3 mmol) was degassed by bubbling argon through it for 10 min. Trifluoroacetic acid (0.064 mL, 0.83 mmol) was then added and the mixture was stirred at room temperature for 20 min, after which time it was diluted with CH_2Cl_2 (50 mL) and then washed with 0.1 M NaOH. The organic layer was dried with anhydrous Na_2SO_4. The solvent was removed under reduced pressure and the unreacted pyrrole was removed by vacuum distillation at room temperature. The resulting viscous liquid was purified by column chromatography [silica gel (100–200 mesh), ethyl acetate/petroleum ether, 15:85; yield: 1.3 g, 45%]. FAB-MS: *m/z* (%) = 356 (50) [M$^+$]. ^{1}H NMR (300 MHz, $CDCl_3$, 25 °C, TMS): δ = 3.85 (s, 3 H), 5.47 (s, 1 H), 5.91 (m, 2 H), 6.15 (m, 2 H), 6.66 (m, 2 H), 6.99 (d, J = 7.2 Hz, 2 H), 7.28 (d, J = 7.8 Hz, 2 H), 7.78 (d, J = 6.6 Hz, 2 H), 7.88 (d, J = 7.2 Hz, 2 H), 7.95 (br. s, 2 H) ppm. $C_{22}H_{20}N_4O$ (356.42): calcd. C 74.14, H 5.66, N 15.72; found C 74.27, H 5.45, N 15.51. This procedure was repeated with **3b** to synthesize **4b**.

Compound 4b: FAB-MS: *m/z* (%) = 384 (50) [M$^+$]. ^{1}H NMR (300 MHz, $CDCl_3$, 25 °C, TMS): δ = 2.36 (s, 6 H), 3.76 (s, 3 H), 5.45 (s, 1 H), 5.91 (m, 2 H), 6.16 (m, 2 H), 6.64 (m, 2 H), 7.29 (d, J = 7.2 Hz, 2 H), 7.61 (s, 2 H), 7.81 (d, J = 6.6 Hz, 2 H), 7.92 (br. s, 2 H) ppm. $C_{24}H_{24}N_4O$ (384.47): 74.97, H 6.29, N 14.57; found C 74.67, H 5.98, N 15.87.

Typical Procedure for the Synthesis of Smaragdyrin: The oxatripyrrane **5a** (0.407 g, 1 mmol) and dipyrromethane **4b** (0.385 g, 1 mmol) were dissolved in dry dichloromethane (250 mL) and the mixture was stirred under nitrogen for 5 min. TFA (0.0068 mL, 0.1 mmol) was added and stirring was continued for a further 90 min. Chloranil (0.738 g, 3 mmol) was added and the reaction mixture was exposed to air and refluxed for a further 90 min. The solvent was then evaporated in vacuo. The residue was purified by column chromatography on basic alumina, and the green band which eluted with dichloromethane gave 0.195 g of **6a** (25% yield), which decomposed above 320 °C. This procedure was applied to synthesize azobenzene–smaragdyrin conjugates **6b–d** and **7a–d** from the corresponding precursors.

Compound 6a: FAB-MS: *m/z* (%) = 754 (100) [M$^+$]. ^{1}H NMR (300 MHz, $CDCl_3$, 25 °C, TMS): δ = 2.74 (s, 6 H), 3.97 (s, 3 H), 7.13 (d, J = 8.8 Hz, 2 H), 7.62 (d, J = 7.8 Hz, 4 H), 8.02 (d, J = 4.2 Hz, 2 H), 8.12 (d, J = 8.4 Hz, 4 H), 8.38 (d, J = 8.4 Hz, 2 H), 8.47 (d, J = 4.2 Hz, 2 H), 8.55 (d, J = 8.4 Hz, 2 H), 8.80 (s, 2 H), 9.03 (d, J = 4.2 Hz, 2 H), 9.42 (d, J = 4.4 Hz, 2 H), 9.49 (d, J = 4.2 Hz, 2 H) ppm. UV/Vis (CH_2Cl_2): λ_{max} ($\varepsilon \times 10^{-4}$ M^{-1} cm^{-1}) = 346 (4), 382 (4), 445 (21.3), 557 (2), 597 (1.7), 641 (1.4), 707 (2.1) nm; (CH_2Cl_2/TFA): λ_{max} ($\varepsilon \times 10^{-4}$ M^{-1} cm^{-1}) = 348 (3.6), 455 (14.5), 482 (sh, 10.8), 615 (1.3), 673 (1.9), 738 (4.3) nm. $C_{50}H_{38}N_6O_2$ (754.88): calcd. C 79.55, H 5.07, N 11.13; found C 79.46, H 5.34, N 11.31.

Compound 6b: FAB-MS: *m/z* (%) = 787 (80) [M$^+$]. ^{1}H NMR (300 MHz, $CDCl_3$, 25 °C, TMS): δ = 3.97 (s, 3 H), 4.12 (s, 6 H), 7.13 (d, J = 9.0 Hz, 2 H), 7.62 (d, J = 7.8 Hz, 4 H), 8.02 (d, J = 4.2 Hz, 2 H), 8.12 (d, J = 8.4 Hz, 4 H), 8.36 (d, J = 8.4 Hz, 2 H), 8.47 (d, J = 4.2 Hz, 2 H), 8.54 (d, J = 8.2 Hz, 2 H), 8.80 (s, 2 H), 9.02 (d, J = 6.0 Hz, 2 H), 9.41 (d, J = 4.2 Hz, 2 H), 9.46 (d, J = 4.2 Hz, 2 H) ppm. UV/Vis (CH_2Cl_2): λ_{max} ($\varepsilon \times 10^{-4}$ M^{-1} cm^{-1}) 342 (3.8), 383 (3.8), 445 (25), 555 (2.1), 595 (1.7), 640 (1.4), 705 (2) nm; (CH_2Cl_2/TFA): λ_{max} ($\varepsilon \times 10^{-4}$ M^{-1} cm^{-1}): 352 (3.4), 453 (15.2), 485 (sh, 10.2), 613 (1.5), 662 (2), 737 (4.7) nm. $C_{50}H_{38}N_6O_4$ (786.88): calcd. C 76.32, H 4.87, N 10.68; found C 76.25, H 4.98, N 10.55.

Compound 6c: FAB-MS: *m/z* (%) = 834 (100) [M$^+$]. ^{1}H NMR (300 MHz, $CDCl_3$, 25 °C, TMS): δ = 1.93 (s, 12 H), 2.65 (s, 6 H), 3.96 (s, 3 H), 7.34 (s, 4 H), 8.12 (d, J = 8.7 Hz, 2 H), 8.38 (m, 4 H), 8.54 (d, J = 8.1 Hz, 4 H), 8.60 (s, 2 H), 9.01 (d, J = 4.2 Hz, 2 H), 9.39 (d, J = 4.2 Hz, 2 H), 9.47 (d, J = 4.2 Hz, 2 H) ppm. UV/Vis (CH_2Cl_2): λ_{max} ($\varepsilon \times 10^{-4}$ M^{-1} cm^{-1}) = 343(6.1), 383 (3.8), 444 (21.5)456 (22.1), 559 (2.7), 602 (2.7), 647 (2.6), 719 (3.6) nm; (CH_2Cl_2/TFA): λ_{max} ($\varepsilon \times 10^{-4}$ M^{-1} cm^{-1}) = 344 (4.9), 456 (18.0), 484 (sh, 11.4), 613 (1.3), 668 (2), 738 (4.8) nm. $C_{54}H_{46}N_6O_2$ (834.37): calcd. C 79.97, H 5.72, N 10.36; found C 79.85, H 5.92, N 10.25.

Compound 6d: FAB-MS: *m/z* (%) = 838 (100) [M$^+$]. ^{1}H NMR (300 MHz, $CDCl_3$, 25 °C, TMS): δ = 1.74 (s, 18 H), 3.87 (s, 3 H), 7.23 (d, J = 9.0 Hz, 2 H), 7.72 (d, J = 7.8 Hz, 4 H), 8.12 (d, J = 4.2 Hz, 2 H), 8.22 (d, J = 8.4 Hz, 4 H), 8.35 (d, J = 8.4 Hz, 2 H), 8.57 (d, J = 4.2 Hz, 2 H), 8.64 (d, J = 8.2 Hz, 2 H), 8.87 (s, 2 H), 9.02 (d, J = 6.0 Hz, 2 H), 9.51 (d, J = 4.2 Hz, 2 H), 9.56 (d, J = 4.2 Hz, 2 H) ppm. UV/Vis (CH_2Cl_2): λ_{max} ($\varepsilon \times 10^{-4}$ M^{-1} cm^{-1}) = 349 (6.9), 445 (28.1), 456 (29.6), 558 (2.7), 601 (2.8), 647 (2.7), 715 (3.8) nm; (CH_2Cl_2/TFA): λ_{max} ($\varepsilon \times 10^{-4}$ M^{-1} cm^{-1}) = 332 (4.5), 456 (16.2), 484 (sh, 11.9), 613 (1.3), 673 (1.9), 738 (4.8) nm. $C_{56}H_{50}N_6O_2$ (838.40): calcd. C 80.16, H 6.01, N 10.02; found C 80.09, H 6.21, N 10.14.

Compound 7a: FAB-MS: *m/z* (%) = 782 (60) [M$^+$]. ^{1}H NMR (300 MHz, $CDCl_3$, 25 °C, TMS): δ = –2.69 (br. s, 1 H), –1.81 (br. s, 1 H), 2.46 (s, 6 H), 2.73 (s, 6 H), 3.86 (s, 3 H), 7.61 (d, J = 7.8 Hz, 4 H), 7.82 (s, 2 H), 8.09 (d, J = 7.8 Hz, 4 H), 8.37 (d, J = 8.1 Hz, 2 H), 8.48 (d, J = 4.2 Hz, 2 H), 8.54 (d, J = 8.4 Hz, 2 H), 8.80 (s, 2 H), 9.02 (d, J = 4.2 Hz, 2 H), 9.40 (d, J = 4.2 Hz, 2 H), 9.49 (d, J = 4.2 Hz, 2 H) ppm. UV/Vis (CH_2Cl_2): λ_{max} ($\varepsilon \times 10^{-4}$ M^{-1} cm^{-1}) =

340 (4), 444 (19.0), 455 (19.0), 556 (1.7), 597 (1.5), 641 (1.2), 707 (1.9) nm; (CH_2Cl_2/TFA): λ_{max} ($\varepsilon \times 10^{-4}$ M^{-1}cm^{-1}) = 343 (4.5), 455 (20), 484 (sh, 14.8), 613 (1.7), 668 (2.5), 738 (6) nm. $C_{52}H_{42}N_6O_2$ (782.93): calcd. C 79.77, H 5.41, N 10.73; found C 79.61, H 5.53, N 10.59.

Compound 7b: FAB-MS: *m*/*z* (%) = 815 (100) [M$^+$]. ^{1}H NMR (300 MHz, $CDCl_3$, 25 °C, TMS): δ = 2.45 (s, 6 H), 3.91 (s, 3 H), 4.14 (s, 6 H), 7.61 (d, *J* = 7.8 Hz, 4 H), 7.82 (s, 2 H), 8.09 (d, *J* = 7.8 Hz, 4 H), 8.37 (d, *J* = 8.1 Hz, 2 H), 8.48 (d, *J* = 4.2 Hz, 2 H), 8.54 (d, *J* = 8.4 Hz, 2 H), 8.80 (s, 2 H), 9.02 (d, *J* = 4.2 Hz, 2 H), 9.39 (d, *J* = 4.2 Hz, 2 H), 9.46 (d, *J* = 4.2 Hz, 2 H) ppm. UV/Vis (CH_2Cl_2): λ_{max} ($\varepsilon \times 10^{-4}$ M^{-1}cm^{-1}) = 346 (5.5), 381 (4.6), 447 (19), 455 (19.4), 558 (1.9), 600 (2.1), 647 (1.9), 712 (2.4) nm; (CH_2Cl_2/TFA): λ_{max} ($\varepsilon \times 10^{-4}$ M^{-1}cm^{-1}) = 349 (4.8), 455 (17.1), 483 (sh, 12.4), 615 (1.8), 661 (2.1), 738 (4.9) nm. $C_{52}H_{42}N_6O_4$ (814.92): calcd. C 76.64, H 5.19, N 10.31; found C 76.73, H 5.05, N 10.12.

Compound 7c: FAB-MS: *m*/*z* (%) = 837 (100) [M$^+$]. ^{1}H NMR (300 MHz, $CDCl_3$, 25 °C, TMS): δ = 1.85 (s, 12 H), 2.56 (s, 6 H), 2.74 (s, 6 H), 3.97 (s, 3 H), 7.35 (s, 4 H), 7.82 (s, 2 H), 8.37 (m, 4 H), 8.54 (d, *J* = 8.4 Hz, 2 H), 8.61 (s, 2 H), 9.01 (d, *J* = 4.2 Hz, 2 H), 9.39 (d, *J* = 4.2 Hz, 2 H), 9.48 (d, *J* = 4.2 Hz, 2 H) ppm. UV/Vis (CH_2Cl_2): λ_{max} ($\varepsilon \times 10^{-4}$ M^{-1}cm^{-1}) = 343 (6.8), 444 (23.5), 456 (23.9), 559 (2.8), 602 (2.9), 647 (2.7), 719 (3.9) nm; (CH_2Cl_2/TFA): λ_{max} ($\varepsilon \times 10^{-4}$ M^{-1}cm^{-1}) = 353 (4.3), 455 (15.2), 483 (sh, 9.7), 613 (1.5), 673 (1.9), 738 (5.2) nm. $C_{56}H_{50}N_6O_2$ (837.04): calcd. C 80.16, H 6.01, N 10.02; found C 80.25, H 5.89, N 10.14.

Compound 7d: FAB-MS: *m*/*z* (%) = 866 (100) [M$^+$]. ^{1}H NMR (300 MHz, $CDCl_3$, 25 °C, TMS): δ = 1.75 (s, 18 H), 2.45 (s, 6 H), 3.91 (s, 3 H), 7.61 (d, *J* = 7.8 Hz, 4 H), 7.82 (s, 2 H), 8.09 (d, *J* = 7.8 Hz, 4 H), 8.37 (d, *J* = 8.1 Hz, 2 H), 8.48 (d, *J* = 4.2 Hz, 2 H), 8.54 (d, *J* = 8.4 Hz, 2 H), 8.80 (s, 2 H), 9.02 (d, *J* = 4.2 Hz, 2 H), 9.39 (d, *J* = 4.2 Hz, 2 H), 9.46 (d, *J* = 4.2 Hz, 2 H) ppm. UV/Vis (CH_2Cl_2): λ_{max} ($\varepsilon \times 10^{-4}$ M^{-1}cm^{-1}) = 344 (8.4), 444 (33.6), 455 (34.7), 558 (3.2), 601 (3.2), 647 (3.0), 717 (4.7) nm; (CH_2Cl_2/TFA): λ_{max} ($\varepsilon \times 10^{-4}$ M^{-1}cm^{-1}) = 348 (3.6), 455 (14.5), 482 (sh, 10.8), 615 (1.3), 673 (1.9), 738 (4.3) nm. $C_{58}H_{54}N_6O_2$ (866.43): calcd. C 80.34, H 6.28, N 9.69; found C 80.42, H 6.12, N 9.74.

Rhodium(I) Complex 8: Compound **6b** (0.030 g, 0.037 mmol) was dissolved in alcohol-free dichloromethane (40 mL). Anhydrous sodium acetate (0.030 g, 0.37 mmol) was added to the solution followed by di-μ-chloridobis[dicarbonylrhodium(I)] (0.020 g, 0.05 mmol), and the mixture was stirred under reflux for 2 h. The solvent was evaporated and the residue was column-chromatographed on silica gel with dichloromethane as eluent. Removal of the solvent gave **8** as a green solid (0.032 g, 95%), which was recrystallized from a dichloromethane/*n*-hexane mixture. FAB-MS: *m*/*z* (%) = 944 (60) [M$^+$]. ^{1}H NMR (300 MHz, $CDCl_3$, 25 °C, TMS): δ = –1.97 (br. s, 2 H), 3.98 (s, 3 H), 4.14 (s, 6 H), 7.13 (d, *J* = 9.0 Hz, 2 H), 7.62 (d, *J* = 7.8 Hz, 4 H), 8.02 (d, *J* = 4.2 Hz, 2 H), 8.12 (d, *J* = 8.4 Hz, 4 H), 8.36 (d, *J* = 8.4 Hz, 2 H), 8.47 (d, *J* = 4.2 Hz, 2 H), 8.54 (m, 2 H), 8.76 (d, *J* = 6.0 Hz, 2 H), 8.83 (s, 2 H), 9.16 (d, *J* = 4.2 Hz, 2 H), 9.49 (m, 2 H) ppm. UV/Vis (CH_2Cl_2): λ_{max} ($\varepsilon \times 10^{-4}$ M^{-1}cm^{-1}) = 297 (3.0), 346 (2.8), 460 (11.3), 478 (8.2), 579 (1.0), 618 (0.9), 638 (1.0), 705 (1.4) nm. $C_{52}H_{37}N_6O_6Rh$ (944.79): calcd. C 66.11, H 3.95, N 8.90; found C 66.42, H 3.78, N 8.79. This procedure was applied for azobenzene–smaragdyrin conjugates **6d**, **7a**, and **7d** to give the rhodium complexes **9**–**11**, respectively.

Compound 9: FAB-MS: *m*/*z* (%) = 996 (50) [M$^+$]. ^{1}H NMR (300 MHz, $CDCl_3$, 25 °C, TMS): δ = –1.92 (br. s, 2 H), δ = 1.74 (s, 18 H), 3.97 (s, 3 H), 7.13 (d, *J* = 9 Hz, 2 H), 7.8–7.85 (m, 4 H), 8.09–8.14 (m, 4 H), 8.22 (d, *J* = 8.1 Hz, 2 H), 8.34 (d, *J* = 8.4 Hz, 2 H), 8.47 (d, *J* = 7.2 Hz, 2 H), 8.58 (m, 2 H), 8.84 (d, *J* = 4.3 Hz, 2 H), 8.89 (s, 2 H), 9.24 (d, *J* = 4.5 Hz, 2 H), 9.54 (m, 2 H) ppm. UV/Vis (CH_2Cl_2): λ_{max} ($\varepsilon \times 10^{-4}$ M^{-1}cm^{-1}) = 300 (2.8), 351 (3.3.), 461 (13.8), 478 (10.5), 579 (1.0), 619 (1.0), 644 (1.0), 707 (1.7) nm. $C_{58}H_{49}N_6O_4Rh$ (996.95): calcd. C 69.87, H 4.95, N 8.43; found C 66.95, H 4.82, N 8.54.

Compound 10: FAB-MS: *m*/*z* (%) = 940 (60) [M$^+$]. ^{1}H NMR (300 MHz, $CDCl_3$, 25 °C, TMS): δ = –1.95 (br. s, 2 H), 2.48 (s, 6 H), 2.74 (s, 6 H), 3.86 (s, 3 H), 7.62 (d, *J* = 7.8 Hz, 4 H), 7.82 (s, 2 H), 8.06 (d, *J* = 4.2 Hz, 2 H), 8.22 (d, *J* = 8.4 Hz, 2 H), 8.36 (d, *J* = 8.4 Hz, 2 H), 8.47 (d, *J* = 4.2 Hz, 2 H), 8.54 (m, 2 H), 8.76 (d, *J* = 6.0 Hz, 2 H), 8.83 (s, 2 H), 9.16 (d, *J* = 4.2 Hz, 2 H), 9.49 (m, 2 H) ppm. UV/Vis (CH_2Cl_2): λ_{max} ($\varepsilon \times 10^{-4}$ M^{-1}cm^{-1}) = 300 (3.5), 345 (4.6), 459 (15.8), 477 (1.8), 578 (1.2), 618 (1.2), 638 (1.8), 705 (2) nm. $C_{54}H_{41}N_6O_4Rh$ (940.85): calcd. C 68.94, H 4.39, N 8.93; found C 68.81, H 4.57, N 8.79.

Compound 11: FAB-MS: *m*/*z* (%) = 1024 (50) [M$^+$]. ^{1}H NMR (300 MHz, $CDCl_3$, 25 °C, TMS): δ = –1.92 (br. s, 2 H), δ = 1.74 (s, 18 H), 2.75 (s, 6 H), 3.86 (s, 3 H), 7.80–7.85 (m, 6 H), 8.10 (d, *J* = 7.8 Hz, 4 H), 8.26 (d, *J* = 8.1 Hz, 2 H), 8.34 (d, *J* = 8.4 Hz, 2 H), 8.47 (d, *J* = 7.2 Hz, 2 H), 8.58 (m, 2 H), 8.84 (d, *J* = 4.3 Hz, 2 H), 9.25 (d, *J* = 4.5 Hz, 2 H), 9.56 (m, 2 H) ppm. UV/Vis (CH_2Cl_2): λ_{max} ($\varepsilon \times 10^{-4}$ M^{-1}cm^{-1}) = 298 (3.8), 344 (4.6), 461 (17.3), 478 (13.2), 578 (1.3) 618 (1.3), 638 (1.3), 705 (2.3) nm. $C_{60}H_{53}N_6O_4Rh$ (1024.32): C70.31, H 5.21, N 8.20; found C 70.31, H 4.97, N 8.48.

X-ray Crystallographic Studies: The crystals were immersed in hydrocarbon oil (Paraton N®), a single crystal selected, mounted on a glass fiber, and placed in the low-temperature N_2 stream. Intensity data were collected at 210 K with a Stoe IPDS2 system utilizing Mo-K_α radiation (λ = 0.71073 Å). The intensities were corrected for Lorentz and polarization effects. The structures were solved by direct methods using the SHELXTL PLUS program system[16] and refined against $|F^2|$ with the program SHELXL-97 using all data.[16]

Table 4. Crystallographic data for azobenzene-containing dipyrromethane **4a** and azobenzene–smaragdyrin conjugate **7a**.

	4a	**7a**
Solvent for crystallization	CH_2Cl_2/hexane	CH_2Cl_2/MeOH
Empirical formula	$C_{22}H_{20}N_4O$	$C_{53}H_{46}N_6O_3$
T [K]	100(2)	100(2)
Crystal system	monoclinic	triclinic
Space group	$P2_1/c$	$P\bar{1}$
V [Å^3]	1808.0(3)	2093.5(5)
a [Å]	7.5731(15)	9.5647(19)
b [Å]	40.991(8)	14.347(3)
c [Å]	5.8368(12)	15.660(3)
α [°]	90	84.033(3)
β [°]	93.79(3)	84.715(3)
γ [°]	90	79.165(3)
Z	4	2
$\rho_{calcd.}$ [Mg m^{-3}]	1.309	1.293
Reflections measured/unique	12055/4473	14034/9945
R (in)	0.0359	0.0370
F(000)	752	860
Limiting indices	$-10 \le h \le 9$	$-12 \le h \le 12$
	$-54 \le k \le 47$	$-19 \le k \le 9$
	$-7 \le l \le 5$	$-20 \le l \le 20$
GoF (F^2)	1.028	1.152
Final *R* indices [$I > 2\sigma I$]		
R_1	0.0559	0.1054
wR_2	0.1274	0.2138
R indices all data		
R_1	0.0755	0.1356
wR_2	0.1374	0.2305

Hydrogen atoms were placed geometrically and refined using a riding model. See Table 4 for further details. CCDC-603853 (**4a**) and -603854 (**7a**) contain the supplementary crystallographic data for this paper. These data can be obtained free of charge from The Cambridge Crystallographic Data Center via www.ccdc.cam.ac.uk/data_request/cif.

Supporting Information (see footnote on the first page of this article): FAB mass, UV/Vis, ^{1}H NMR spectra of selected compounds.

Acknowledgments

This work was supported by grants from the Department of Science and Technology (DST) and the Council of Scientific and Industrial Research (CSIR), Government of India, New Delhi. S. G., V. P. R., and J. S. thank CSIR for fellowships.

[1] a) N. Liu, D. R. Dunphy, M. A. Rodriguez, S. Singer, J. Brinker, *Chem. Commun.* **2003**, 1144–1145; b) Y. Yu, T. Ikeda, *Macromol. Chem. Phys.* **2005**, *206*, 1705–1708.
[2] a) O. Srinivas, N. Mitra, A. Surolia, N. Jayaraman, *J. Am. Chem. Soc.* **2002**, *124*, 2124–2125; b) X. Liu, M. Jiang, *Angew. Chem. Int. Ed.* **2006**, *45*, 3846–3850.
[3] a) L. Brzozowski, E. H. Sargent, *J. Mater. Sci.* **2001**, *12*, 483–489; b) A. Natansohn, P. Rochon, *Adv. Mater.* **1999**, *11*, 1387–1391.
[4] Y. Norikane, N. Tamaoki, *Org. Lett.* **2004**, *6*, 2595–2598.
[5] a) M. Autret, M. L. Plouzennec, C. Moinet, G. Simonneaux, *J. Chem. Soc., Chem. Commun.* **1994**, 1169–1170; b) C. A. Hunter, L. D. Sarson, *Tetrahedron Lett.* **1996**, *37*, 699–702; c) D. R. Reddy, B. G. Maiya, *Chem. Commun.* **2001**, 117–118; d) T. E. O. Screen, I. M. Blake, L. H. Rees, W. Clegg, S. J. Borwick, H. L. Anderson, *J. Chem. Soc., Perkin Trans. 1* **2002**, 320–329.
[6] J. L. Rodríguez-Redondo, Á. Sastre-Santos, F. Fernández-Lázaro, D. Soares, G. C. Azzellini, B. Elliott, L. Echegoyen, *Chem. Commun.* **2006**, 1265–1267.
[7] T. Muraoka, K. Kinbara, T. Aida, *Nature* **2006**, *440*, 512–515.
[8] T. K. Chandrashekar, S. Venkatraman, *Acc. Chem. Res.* **2003**, *36*, 676–691.
[9] S. J. Narayanan, B. Sridevi, T. K. Chandrashekar, U. Englich, K. R-Senge, *Org. Lett.* **1999**, *1*, 587–590.
[10] a) S. Venkatraman, R. Kumar, J. Sankar, T. K. Chandrashekar, K. Sendhil, C. Vijayan, A. Kelling, M. O. Senge, *Chem. Eur. J.* **2004**, *10*, 1423–1432; b) R. Kumar, R. Misra, V. Prabhuraja, T. K. Chandrashekar, *Chem. Eur. J.* **2005**, *11*, 5695–5707; c) R. Misra, R. Kumar, V. Prabhuraja, T. K. Chandrashekar, *J. Photochem. Photobiol.* **2005**, *175*, 108–117.
[11] a) S. J. Narayanan, B. Sridevi, T. K. Chandrashekar, U. Englich, K. R. Senge, *Inorg. Chem.* **2001**, *40*, 1637–1645; b) B. Sridevi, S. J. Narayanan, R. Rao, T. K. Chandrashekar, U. Englich, K. R. Senge, *Inorg. Chem.* **2000**, *39*, 3669–3677.
[12] M. Han, M. Hara, *J. Am. Chem. Soc.* **2005**, *127*, 10951–10955.
[13] M. V. Peters, R. Goddard, S. Hecht, *J. Org. Chem.*, DOI: 10.1021/jo0612877.
[14] B. Sridevi, S. J. Narayanan, A. Srinivasan, M. V. Reddy, T. K. Chandrashekar, *J. Porphyrins Phthalocyanines* **1998**, *2*, 69–78.
[15] D. C. Gowda, B. Mahesh, S. Gowda, *Ind. J. Chem. Sect. B* **2001**, *40*, 75–77.
[16] a) b) G. M. Sheldrick, *SHELXS-93f*, University of Göttingen, Germany, **1993**; G. M. Sheldrick, *SHELXL-97*, University of Göttingen, Germany, **1997**.

Received: August 16, 2006
Published Online: November 17, 2006

